Modeling Multiple Hemodynamic Responses in Event-Related Functional MRI Experiments

F. Kruggel, S. Zysset and D. Y. von Cramon
Max-Planck-Institute of Cognitive Neuroscience
Stephanstraße 1, 04103 Leipzig, Germany
{*kruggel, zysset, cramon*}*@cns.mpg.de*

Abstract

This paper discusses issues of analyzing multiple responses in fMRI data obtained in event-related experimental studies of human working memory. A nonlinear regression context is proposed to quantitatively compare stimulation parameters and observed hemodynamic responses.

1 Introduction

Functional magnetic resonance imaging (fMRI, [1]) has become one of the major methods for investigating brain function in cognitive science. Most fMRI studies apply the blood-oxygen-level-dependent (BOLD) effect which is related to temporal changes of the oxygen content in venules and so only indirectly linked to neuronal activation via metabolic processes. The observed hemodynamic response (HR) is typically delayed by 3-5s and dispersed by 1.5-2.5s with respect to a brief stimulus, and perhaps also displaced with respect to the activation site. In addition, the effect is rather small, and data are noisy. These facts complicate fMRI data analysis and led to a focus on the problem of signal detection during the last few years: to determine the site of brain activation in relation to a certain experimental stimulus.

Recently, event-related experimental designs were introduced (ER-fMRI). An event (or trial) is understood as a "self-contained behavioural/perceptual unit which is temporally limited" [2]. Such designs allow the randomized presentation of behavioural trials and the study of responses to a specific stimulation separately. As a consequence, there is an increasing interest in describing the timecourse of the HR [3]: how much can be inferred from the HR shape characteristics about the underlying neuronal activation?

In cognitive studies of human memory, a single trial often consists of two (or more) individual stimuli, which can be separated in time. Each stimulus is expected to elicit HRs, thus two (or more) responses may occur during a single trial. More specifically, it is of interest, whether activated brain regions contribute to *either* the first *or* the second *or* both phases *or* are even active throughout the delay phase.

This paper discusses issues of detecting and describing single and multiple responses in relation to the experimental stimulus. In the next section, we describe a prototypical memory experiment used to illustrate the techniques discussed in this paper. Then we apply progressively finer techniques of signal description using linear univariate regression, selective averaging of single trials and nonlinear multiple regression. A final discussion focuses on limitations and pitfalls of the methods applied here.

2 Experimental Paradigm

We considered a classical Sternberg paradigm [4] with varied sets. Memory lists were composed of consonants of the alphabet, excluding the letter Y. A subspan set size of 3, 4, 5 and 6 letters was presented visually for 2s (cue phase). After a variable delay length (2.0s, 3.2s, 4.1s, 5.2s, 6.2s, 7.0s) a probe letter appeared (probe phase). Subjects had to decide if the probe letter belonged to the previously presented set. A hit response was given by pressing a button with the ring finger (resp. the middle finger for a foil response). 48 trial combinations (4 (set sizes) x 6 (delay length) x 2 (hit/foil manipulation)) were presented randomly in a single run.

For fMRI scanning, a single-shot EPI sequence was applied (TR 1s, 8 slices parallel to the AC-PC plane, 64x64 voxels, 192mm field-of-view, 5mm slice thickness, 3mm gap) in an event-related experimental paradigm with an inter-trial interval of 18s, corresponding to 14.4min scanning time per run. 7 subjects took part in this study, 2 of which completed 3 runs, the

0-7803-5871-6/99/$10.00

other 5 completed 4 runs.
Reaction times (relative to the probe phase) and responses were recorded along with the stimulation. Results for all subjects were pooled, incorrect (N=34) and missed (N=20) responses were excluded from a total of N=1244 trials (4.3%). Using a general linear model for Poisson-distributed data, a mean reaction time (RT) of 672.8 ± 5.3 ms, a RT decrease by delay time of -18.1 ± 0.6 ms, and a RT increase by set size of 39.6 ± 0.9 ms was found. Hits were -54.6 ± 2.0 ms faster than foils, a slight RT decrease of 39 ms during the experiment was interpreted as an optimization of the task.

3 fMRI Data Processing

Data analysis consisted of several steps: preprocessing, activation detection using voxelwise linear regression, selective averaging of HRs in regions-of-interest (ROIs), and shape analysis of the hemodynamic response by nonlinear regression. These steps are now described in detail.

3.1 Preprocessing

A standard preprocessing scheme was applied to the raw fMRI datasets [5]: correction for intensity differences between scans, correction for subject motion within and between scans, baseline estimation using low-pass filtering in the temporal domain and subtraction of the estimated baseline from the data, and lowpass-filtering in the temporal domain for reduction of physiological and system noise, including a band between 0.8 and 2.5 times the fundamental stimulation frequency.

3.2 Linear Regression Analysis

The next data analysis step consisted of the detection of activated areas in the brain. For statistical analysis, two regressors were constructed as follows (see Fig. 1): timesteps 0-2 and 16-17 were coded as baseline, timesteps 5-7 as activated for the cue regressor (corresponding to the cue phase), two timesteps around the experimental delay time plus 5.5s as activated (for the probe regressor), the other timesteps were excluded.
Functional activation was detected by performing voxelwise univariate regression with these regressors [6], conversion of the regression coefficients into z values, and thresholding of the corresponding z-map by a score of 10, and assessment of the activated regions for their significance on the basis of their spatial extent [7]. We defined regions-of-interest (ROIs) as the 6 most highly activated 4-connected voxels around local maxima in the z-map. We selected 8 ROIs which were found at homologous anatomical sites in at least 5 of the 7 subjects incorporated in this study. ROIs at their prototypical locations are shown in Fig. 3 and listed in Tab. 2.

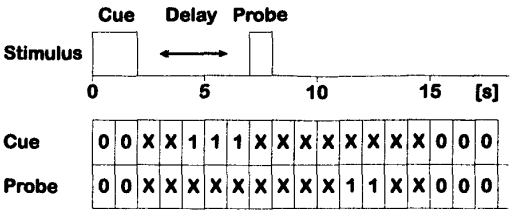

Figure 1: Stimulation scheme and corresponding regressors for the cue and probe phase.

ROIs differed in their activity during both experimental phases. "Input-oriented" areas (such as MTG_L, TOG_L, PPC_R) correlated higher with the cue phase, while "output-oriented" areas (MC_L) were mostly active during the probe phase. A fronto (MFG_L, PCG_L, PCG_R) - parietal (PPC_L, SIP_L) network was active during both phases. The SMA also took part in both phases.

3.3 Selective Averaging

Regression analysis was performed to detect functional activation. This procedure, however, did not allow the discrimination between a *double* response (once during cue, once during probe phase) and a *continued* activation.
An obvious next step was to compute power spectra of the timeseries and to check the relation of the power at the stimulation frequency vs. its first harmonic. In activated regions of experiments involving a single stimulus, a typical ratio of 10:1 was found. For ROIs of this experiment, ratios between 10:1 and 10:3 were computed, i.e. in all regions, the contribution

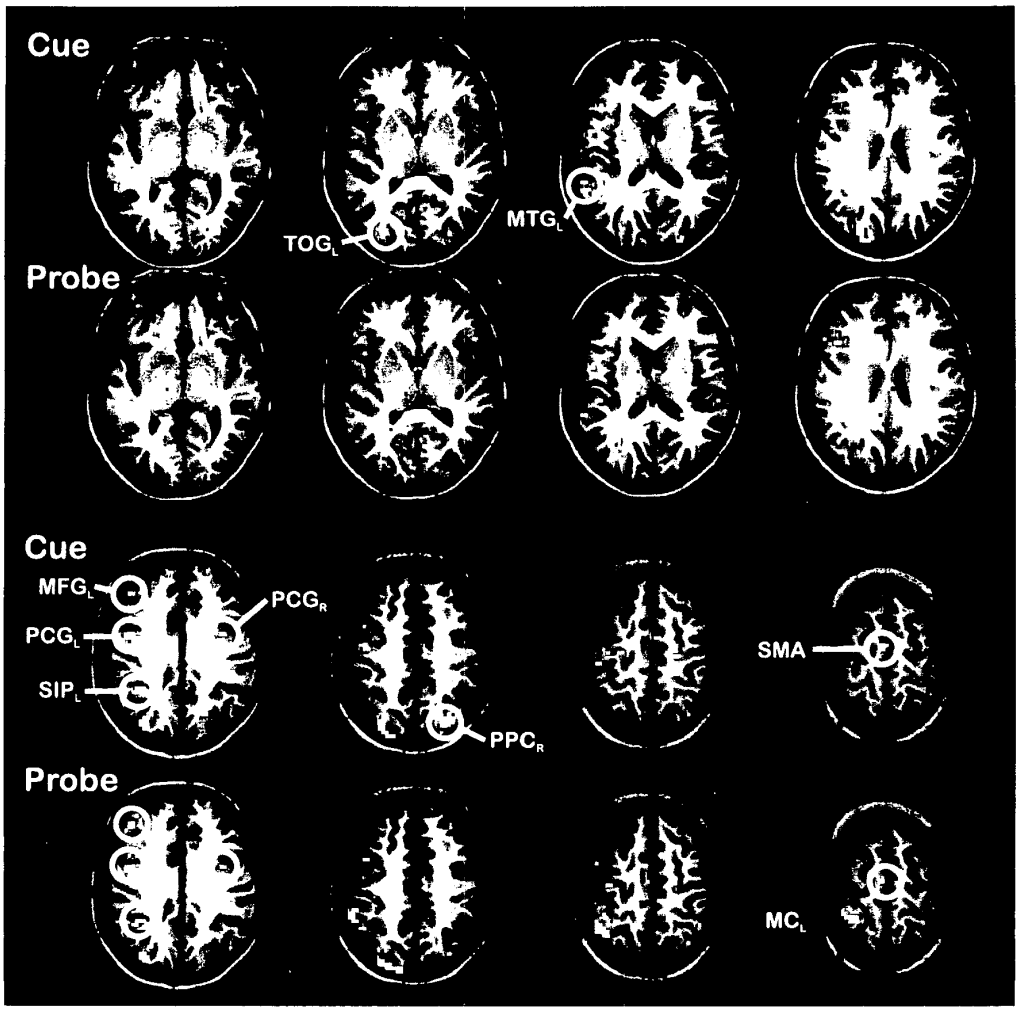

Figure 3: Univariate regression analysis in a sample subject: significantly activated regions related to the cue phase are shown in row 1 and 3, during probe phase in row 2 and 4. Properties of ROIs are color-coded by their amount of contribution (green: cue, red: probe, yellow: both phases).

ROI	Anatomical Site	Cue Phase	Probe Phase
MTG_L	left medio-temporal gyrus	+	-
TOG_L	left transverse occipital gyrus	+	-
PPC_R	right posterior parietal cortex	+	-
MFG_L	left middle frontal gyrus	+	+
PCG_L	left precentral gyrus	+	+
PCG_R	right precentral gyrus	+	+
SIP_L	(banks) of the left sulcus intraparietalis	+	+
SMA	supplementary motor area	+	+
MC_L	left motor cortex	-	+

Table 2: Anatomical sites of ROIs and their participation during the cue and probe phase.

of the stimulation frequency was predominant. Another simple option to learn more about the temporal characteristic is selective averaging of trials with the same stimulation characteristics [8]. We formed averages within ROIs defined above and across all trials of the same delay time manipulations. Results for a sample subject were compiled in Fig. 2. We found that *all* regions were active during cue and probe phase. The activation amount in both phases differed from region to region and corresponded roughly to the results from regression analysis compiled in Tab. 2. No region showed a sustained activation throughout the delay phase. Secondary visual areas (such as MTG_L and TOG_L) showed an activation drop during the delay phase, although visual stimulation was continued in the form of a fixation point. However, all activations overlapped strongly in both phases for delay times of less than 4s.

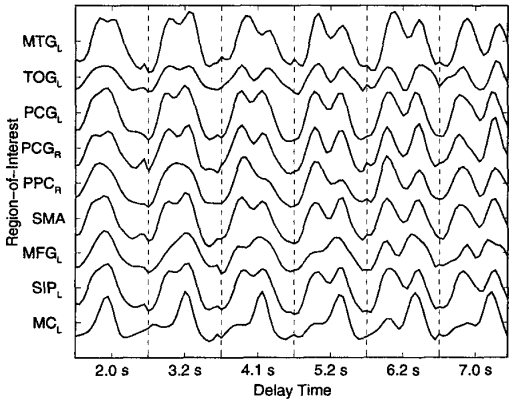

Figure 2: Averaged timecourses for ROIs defined in Tab. 2, selected from trials of the same delay time.

3.4 Shape Analysis

Selective averaging was used to visualize temporal properties of the HR timecourse in different ROIs. To describe HR properties quantitatively with respect to stimulation parameters, we set up a nonlinear regression model [9]. Model and results are now described in more detail.

Nonlinear Regression Model

We consider acquired functional data $\mathbf{y}$, collected at $k = 6$ voxel sites of predefined ROIs throughout $l = 18$ timesteps of $m = \{144, 192\}$ trials. Functional data are modeled as a sum of a deterministic function $g(\cdot)$ and a stochastic part $\boldsymbol{\epsilon}$:

$$\mathbf{y} = g(\mathbf{t}, \boldsymbol{\beta}) + \boldsymbol{\epsilon},$$

where $\mathbf{t}$ corresponds to the discrete timesteps and $\boldsymbol{\beta}$ to the $p = 6$-dimensional vector of model parameters of a sum of two Gaussian functions:

$$g(t, \boldsymbol{\beta}) = \beta_0 \exp\left[-\frac{(t-\beta_2)^2}{2\beta_1^2}\right] + \beta_3 \exp\left[-\frac{(t-\beta_5)^2}{2\beta_4^2}\right]$$

We denote the components of $\boldsymbol{\beta}$ as β_0, β_3: gain (the "height" of both HRs), β_1, β_4: dispersion (proportional to the duration of the HRs), β_2, β_5: lag (the time delay from stimulation onset to the HR maximum). Note that parameters $\boldsymbol{\beta}$ are functions of the stimulation context of a given trial.

We assume that the stochastic part is independent of the signal and stationary with respect to time, and its elements are normally distributed with a nonsingular covariance matrix $\mathbf{V}$: $\boldsymbol{\epsilon} \sim N_n(0, \mathbf{V})$, where $n = k * l * m$ corresponds to the number of data points. For reasons of simplicity, we set $V = I$ in this study. A more advanced formulation may incorporate AR(1) autocorrelation in time and space [10].

We find the ML estimate $\hat{\boldsymbol{\beta}}$ of our model parameters as the vector $\boldsymbol{\beta}$ that minimizes the quantity:

$$\arg\min_{\beta}(\boldsymbol{\epsilon}^T \mathbf{V}^{-1} \boldsymbol{\epsilon}), \quad \text{where} \quad \boldsymbol{\epsilon} = \mathbf{y} - g(\mathbf{t}, \boldsymbol{\beta}).$$

This nonlinear minimization problem was solved using Powells algorithm [11].

Using a first-order linear model, we can derive confidence limits for the estimation from the inverse of the Fisher information matrix $\mathbf{F}$:

$$\hat{\boldsymbol{\beta}} \sim N(\boldsymbol{\beta}, \mathbf{F}_{\boldsymbol{\beta}}^{-1}), \quad \text{where} \quad \mathbf{F}_{\boldsymbol{\beta}} = \mathbf{G}_{\boldsymbol{\beta}} \mathbf{V}^{-1} \mathbf{G}_{\boldsymbol{\beta}}^T,$$

and $\mathbf{G}_{\boldsymbol{\beta}}$ denotes the Jacobian matrix of $g(\cdot)$ with respect to $\boldsymbol{\beta}$. A simple measure for the goodness-of-fit (GOF) is given by:

$$GOF = 1 - \frac{\boldsymbol{\epsilon}^T \mathbf{V}^{-1} \boldsymbol{\epsilon}}{\mathbf{y}^T \mathbf{V}^{-1} \mathbf{y}}, \quad GOF \in [0, 1],$$

with 1 denoting a perfect fit. A more complex measure is derived for the F-statistics, following a suggestion of Hartley (see [9]):

$$F_{p,n-p,\alpha} \approx \frac{(n-p)}{p} \frac{\boldsymbol{\epsilon}^T \mathbf{P} \boldsymbol{\epsilon}}{\boldsymbol{\epsilon}^T (\mathbf{I}_n - \mathbf{P}) \boldsymbol{\epsilon}},$$
$$\text{using} \quad \mathbf{P} = \mathbf{G}_{\boldsymbol{\beta}} \mathbf{F}_{\boldsymbol{\beta}}^{-1} \mathbf{G}_{\boldsymbol{\beta}}^T,$$

where n corresponds to the number of data points, p to the number of parameters, and $\mathbf{I}_n$ is the (n,n) identity matrix.

Results

We tested different models for the dependency of $\boldsymbol{\beta}$ on the stimulation parameters with this regression context. The most simple model used independent gains (β_0, β_3) for both phases, a fixed dispersion ($\beta_1 = \beta_4 = 1.8$s), and a lag time of the second phase, which followed the first one by the delay time manipulation d plus 2s for the duration of the first stimulation phase: $\beta_5 = \beta_2 + d + 2$s.

This model resulted in GOF values of 0.40-0.55 for all ROIs in all subjects. We excluded 10-15% of the trials where subjects missed to respond or gross misfits due to artifacts in the data were noticed. Using the fitted parameters as starting values, we successively refined this model by introducing additional dependencies on the stimulation parameters. Best fits, as given by GOF values and Akaike's information criterion, were found for the following model:

- the gain of the first response had a constant part, but depended on the experiment duration t and the set size s: $\beta_0 = a_0 + a_1 * t + a_2 * s$.
- the dispersion of the first response had a constant part, but depended on the set size: $\beta_1 = 1.8 + a_3 * s$.
- the lag of the first response had a constant part, but depended on the set size: $\beta_2 = a_4 + a_5 * s$.
- the gain of the second response had a constant part, but depended on the experiment duration and the delay time d: $\beta_3 = a_6 + a_1 * t + a_7 * d$.
- the dispersion of the second response had a constant part, but depended on the set size: $\beta_4 = 1.8 + a_8 * s$.
- the lag of the second response had a constant part, but depended on the delay time, the set size and the hit/foil manipulation h: $\beta_5 = a_4 + d + 2 + a_9 * s + a_{10} * h$.

ROI	MTG_L	TOG_L	PPC_R	MFG_L
GOF	0.768	0.863	0.798	0.726
a_0	121.7	124.5	194.2	111.8
a_1	-0.317	-0.282	-0.543	-0.404
a_2	8.25	14.57	13.16	4.62
a_3	0.128	0.097	0.093	0.152
a_4	4.63	3.93	4.54	4.26
a_5	0.111	0.260	0.312	0.184
a_6	120.2	56.6	127.4	99.6
a_7	3.70	5.96	4.36	4.98
a_8	0.094	0.300	0.219	0.207
a_9	0.000	0.000	0.130	0.031
a_{10}	-0.252	-0.000	-0.001	-0.101

ROI	PCG_L	PCG_R	SIP_L	SMA	MC_L
GOF	0.890	0.776	0.893	0.819	0.830
a_0	100.1	159.6	74.3	115.6	69.3
a_1	-0.456	-0.643	-0.254	-0.406	-1.061
a_2	19.18	3.22	13.73	16.51	4.57
a_3	0.175	0.156	0.164	0.199	0.129
a_4	3.84	4.03	4.15	3.87	4.68
a_5	0.446	0.298	0.379	0.376	0.322
a_6	132.8	125.4	83.7	140.3	272.7
a_7	3.95	3.25	4.95	6.50	1.92
a_8	0.206	0.187	0.189	0.223	0.096
a_9	0.054	0.062	0.000	0.068	0.033
a_{10}	-0.000	-0.051	-0.016	-0.499	-0.136

Table 1: Goodness-of-fit and fitted parameters of nonlinear regression analysis in ROIs from a sample subject. For the meaning of these parameters, refer to the text section above.

GOF values for this 11 parameter model ranged between 0.70 and 0.91, and were rendered significant ($\alpha < 0.05$) by the F statistics. Results for a sample subject are shown in Tab. 1. Fitted parameters for the other subjects were similar. We interpreted results as follows:

- all ROIs were active during both phases of a trial (parameters a_0, a_6).

- a slight decrease of all activations with experiment time (i.e. per trial number) was noticed (parameter a_1). This may be interpreted as a habituation or optimization effect.

- the cue phase response depended on the set size manipulation only. The highest relative gain increase per set item was found for ROIs PCG_L, SIP_L and SMA (ratio a_2/a_0), and a low increase for ROIs MFG_L, MTG_L, PCG_R and MC_L. Lag and dispersion also increase with set size (a_3 resp. a_5). These effects may be attributed either to a longer processing time with increasing set size or the consequence of a higher energy consumption.

- the lag of the probe phase response followed the probe phase stimulation strictly, and the gain was independent of the set size.

- an increasing set size led to a slightly longer duration (a_8) and a temporally shifted peak (a_9) of the probe response, which is in the order of the reaction time differences found for the behavioural evaluation.

- lags of the probe response for hits were slightly faster than for foils (a_{10}), which was in accordance with the behavioural evaluation.

- however, due to comparatively high error ranges for parameters a_8-a_{10} (not shown here for space restrictions), a characterization of ROIs by the amount of dependency on the stimulation parameters could not be made.

- the ratio of the cue and probe phase gains (a_0/a_6) indicated a higher involvement of ROIs MTG_L, TOG_L, PPC_R during the cue phase, a predominant involvement of ROIs SMA and MC_L during the probe phase, while ROIs MFG_L, PCG_L, PCG_R and SIP_L responded approximately equally in both phases.

4 Discussion

Using a nonlinear regression scheme to model the HR timecourse in predefined brain regions, we were able to quantify the activation of a region during different phases of an experimental trial and to discriminate their dependency on the stimulation content. A Gaussian model function for the HR offers the benefit of yielding "physiologically meaningful" parameters like gain, lag and dispersion, which may easily be understood in terms of the experimental stimulation. Regions may either be defined by prior knowledge, neurofunctional interest or result from an analysis using "classical" signal detection methods such as univariate regression. Once homologous ROIs have been defined in a group of subjects, it is easy to set up nonlinear models described here. Given reasonable starting parameters, simple nonlinear optimization methods are sufficient to solve models. Because only a small subset of the raw data is entered into analysis, results for a given model are available within a few seconds of computation time.

Other physiological influences than stimulus variables model the HR shape. The timecourse of the BOLD effect is rate-limited, i.e. the slope has an upper bound. Thus, experimental manipulations that introduce a stronger activation lead to a temporal shift of the lag and to a more dispersed HR shape. A slight gain decrease was found in all ROIs during the experiment, indicating habituation or an optimization process. With short delay times, both HRs merge, and an assignment of parameters to each component is arbitrary. For this reason, we decided to model the *whole* timeseries instead of modeling each trial separately.

With a rather high number of influences, selection of a proper model is a problem. We found a stepwise approach to be most proficient: starting from a rather simple model including "hard" effects (such as the delay time manipulation), we then introduced physiological constraints, and finally, other parameters of the experimental design. Currently, this process is experience-driven and not exhaustive. Note that we also restricted to linear dependencies on stimulation parameters.

Neurobiological implications of the study presented here will be discussed in a different publication. Results are well in accordance with recently published data of studies in human working memory [12, 13]. However, the nonlinear regression analysis proposed in this paper yielded results beyond standard fMRI analysis and allowed describing brain activation on a much finer level.

Increasingly complex experimental designs require more elaborate statistical procedures to quantitatively compare between stimulus and response. The proposed nonlinear modeling context for the hemodynamic response offers a high degree of flexibility. It may serve as another tool to face the challange of understanding brain function.

References

[1] Belliveau JW, Kennedy DN, McKinstry RC, Buchbinder BR, Weisskoff RM, Cohen MS, Vevea JM, Brady TJ, Rosen BR (1991) *Functional mapping of the human visual cortex by magnetic resonance imaging.* Science 254, 716-719.

[2] Zarahn E, Aguirre G, D'Esposito M (1997) *A trial-based experimental design for fMRI.* NeuroImage 6, 122-138.

[3] Rajapakse JC, Kruggel F (1997) *Neuronal and hemodynamic events from functional MRI time-series: a computational model.* In: N. Kasabov, R. Kozma, K. Ko, R. O'Shea, G. Coghill, T. Gedeon (Eds.), Progress in Connectionist-Based Information Systems (ICONIP 97), p. 30-34, Singapore: Springer.

[4] Sternberg S (1966) *High-speed scanning in human memory.* Science 153, 652-654.

[5] Kruggel F, Descombes X, von Cramon DY (1998) *Preprocessing of fMR datasets.* Workshop on Biomedical Image Analysis (Santa Barbara), p. 211-220. Los Alamitos: IEEE Computer Press.

[6] Rajapakse JC, Kruggel F, Maisog J, von Cramon DY (1998) *Modeling hemodynamic response for analysis of functional MRI time-series.* Human Brain Mapping 6, 283-300.

[7] Friston KJ, Worsley KJ, Frackowiak RSJ, Mazziotta JC, Evans AC (1994) *Assessing the significance of focal activations using their spatial extent.* Human Brain Mapping 1, 210-220.

[8] Dale AM, Buckner RL (1997) *Selective averaging of rapidly presented individual trials using fMRI.* Human Brain Mapping 5, 329-340.

[9] Seber GAF, Wild CJ (1989) *Nonlinear Regression.* New York: Wiley.

[10] Kruggel F, von Cramon DY (1999) *Modeling the hemodynamic response in single trial fMRI experiments.* Magnetic Resonance in Medicine, in print.

[11] Press WH, Teukolsky SA, Vetterling WT, Flannery BP (1992) *Numerical Recipes in C.* Cambridge: Cambridge University Press.

[12] Smith EE, Jonides J (1998) *Neuroimaging analysis of human working memory.* Proceedings of the National Academy of Sciences 95, 12061-12068.

[13] Rypma B, Prabhakaran V, Desmond JE, Glover GH, Gabrieli JDE (1999) *Load-dependent roles of frontal brain regions in the maintainance of working memory.* NeuroImage 9, 216-226.